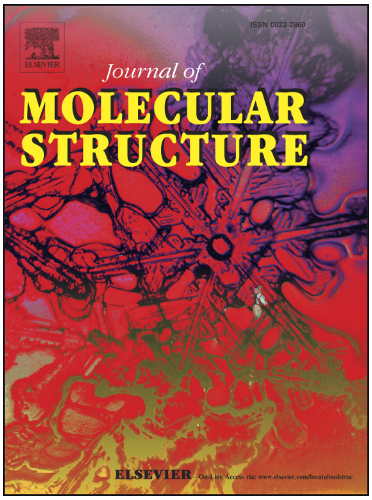

Synthesis, characterization and X-ray crystal structures of Vanadium(IV), Cobalt(III), Copper(II) and Zinc(II) complexes derived from an asymmetric bidentate Schiff-base ligand at ambient temperature

Mahsa Khorshidifard, Hadi Amiri Rudbari, Zahra Kazemi-Delikani, Valiollah Mirkhani, Reza Azadbakht

PII: S0022-2860(14)01084-9
DOI: http://dx.doi.org/10.1016/j.molstruc.2014.10.071
Reference: MOLSTR 21067

To appear in: *Journal of Molecular Structure*

Received Date: 10 September 2014
Revised Date: 24 October 2014
Accepted Date: 28 October 2014

Please cite this article as: M. Khorshidifard, H.A. Rudbari, Z. Kazemi-Delikani, V. Mirkhani, R. Azadbakht, Synthesis, characterization and X-ray crystal structures of Vanadium(IV), Cobalt(III), Copper(II) and Zinc(II) complexes derived from an asymmetric bidentate Schiff-base ligand at ambient temperature, *Journal of Molecular Structure* (2014), doi: http://dx.doi.org/10.1016/j.molstruc.2014.10.071

Synthesis, characterization and X-ray crystal structures of Vanadium(IV), Cobalt(III), Copper(II) and Zinc(II) complexes derived from an asymmetric bidentate Schiff-base ligand at ambient temperature

Mahsa Khorshidifard[a], Hadi Amiri Rudbari[a,]*, Zahra Kazemi-Delikani[a], Valiollah Mirkhani[a], Reza Azadbakht[b]

[a]*Department of Chemistry, University of Isfahan, Isfahan 81746-73441, Iran*

[b]*Department of Chemistry, Payame Noor University, Tehran, Iran*

* Corresponding author. Tel.: +98 31 37932712.

E-mail address: h.a.rudbari@sci.ui.ac.ir; hamiri1358@gmail.com (H. Amiri Rudbari)

Abstract

An asymmetric bidentate Schiff-base ligand (**HL**: 2-((allylimino)methyl)phenol) was prepared from reaction of salicylaldehyde and Allylamine. Vanadium(IV), Cobalt(III), Copper(II) and Zinc(II) complexes, **VOL_2**, **CoL_3, CuL_2 and ZnL_2** were synthesized from the reaction of $VO(acac)_2$, $CoCl_2.6H_2O$, $CuCl_2.2H_2O$ and $Zn(NO_3)_2.6H_2O$ with the bidentate Schiff base ligand (**HL**: 2-allyliminomethyl-phenol) in methanol at ambient temperature. The ligand and its metal complexes were characterized by elemental analysis (CHN), FT-IR spectroscopy. In addition, ^{1}H and ^{13}C NMR techniques were employed for characterization of the ligand (**HL)** and diamagnetic complex **ZnL_2**. The molecular structures of all complexes were determined by single crystal X-ray diffraction technique. In the **ZnL_2** and **CuL_2** complexes, the metal ion is coordinated by two nitrogen and two oxygen atoms from two Schiff base ligands in an approximately square planar *trans*-[MN2O2] coordination geometry. In the vanadium(IV) complex, **VOL_2**, the vanadium center in this structure has a distorted tetragonal pyramidal N2O3 coordination sphere and for Cobalt(III) complex, **CoL_3**, the Co^{III} ion is six coordinated by three bidentate Schiff base ligands in a distorted octahedral environment.

Keywords

Bidentate Schiff base ligand; Schiff base complexes; X-ray crystal structure; Ambient temperature

1. Introduction

Considerable interest exists in the coordination chemistry of transition metals with Schiff bases due to the wide range of applications and structural aspects of the resulting complexes [1–5]. Salen ligands and the related salophen ligands are of interest to a wide variety of chemists [6-9]. Salen complexes have been used as catalytically active materials to develop surface modified electrodes for sensor applications [10,11]. It has been suggested that the azomethine linkage is responsible for the biological activities of Schiff bases such as, antitumor, antibacterial, antifungal and herbicidal activities [12–16]. Although, a lot of Schiff bases with different structures have been synthesized and characterized, however, less attention has been focused on the Schiff base ligands and complexes with amines containing terminal allyl group [16,17].

The compounds with terminal allyl group can covalently attach on an insoluble support and use as heterogeneous catalysts instead of homogeneous catalysts [18-21]. For example: Garcia *et al*, anchored a series of vanadyl Schiff base complexes having a terminal carbon–carbon double on silicas as solid enantioselective catalysts for formation of cyanohydrins [18]. From the sustainable and green chemistry point of view, heterogeneous catalysts would be attractive since they offer the advantages of easy catalyst separation, possible catalyst recycle and sometimes high activity and selectivity.

As part of our research program on the synthesis and characterization of Schiff base ligands and complexes [22-30], in this paper, the authors synthesized a bidentate Schiff base ligand derived from salicylaldehyde and Allylamine (**HL**: 2-((allylimino)methyl)phenol). In order to investigate the coordination modes of this ligand, Vanadium(IV), Cobalt(III), Copper(II) and Zinc(II) complexes were synthesized and characterized by the FT-IR, ^{1}H NMR, ^{13}C NMR, elemental analysis and X-ray crystallography.

2. Experimental section

2.2.Chemicals and instrumentation

All the chemicals were purchased from Merck Co. and used without further purification. The FT-IR spectrum was recorded on a JASCO, FT/IR-6300 spectrometer (4000–400 cm^{-1}) in KBr pellets. ^{1}H and ^{13}C NMR spectra were recorded on a Bruker Avance 400 spectrometer using $CDCl_3$ as solvents for the ligand and Zinc(II) complex. The elemental analysis was performed on Leco, CHNS-932 and Perkin-Elmer 7300 DV elemental analyzers.

2.2 Single crystal diffraction studies

X-ray data for complexes were collected on a STOE IPDS-II diffractometer with graphite monochromated Mo-Kα radiation. For **ZnL$_2$**, a dark yellow block crystal, for **CoL$_3$**, a red needle crystal, for **VOL$_2$**, a yellow needle crystal and for **CuL$_2$**, a green crystal was chosen using a polarizing microscope and they were mounted on a glass fiber which was used for data collection. Cell constants and an orientation matrix for data collection were obtained by least-squares refinement of diffraction data from 3095 for **ZnL$_2$**, 4780 for **CoL$_3$**, 3335 for **VOL$_2$** and 3108 for **CuL$_2$** unique reflections. Data were collected at a temperature of 298(2) in a series of ω scans in 1° oscillations and integrated using the Stöe X-AREA [31] software package. A numerical absorption correction was applied using the X-RED [28] and X-SHAPE [32] software's. The data were corrected for Lorentz and Polarizing effects. The structures were solved by direct methods using SIR2004 [33]. The non hydrogen atoms were refined anisotropically by the full matrix least squares method on F^2 using SHELXL [34]. All hydrogen atoms were added at ideal positions and constrained to ride on their parent atoms. Crystallographic data for complexes are listed in Table 2. Selected bond distances and angles are summarized in Table 3.

2.3.Synthesis of Schiff-base ligand (HL**: 2-((allylimino)methyl)phenol**)

Schiff base ligand, **HL**, was synthesized according to the slightly modified literature procedure [16]. This ligand has been synthesized at reflux condition by Johnson *et al*, but here we synthesized this ligand at room temperature with higher yield in methanol or chloroform as solvent (Scheme 1).

Allylamine (IUPAC name: 3-amino-prop-1-ene) (10 mmol) was dissolved in 30 ml of absolute methanol or chloroform and added slowly to a stirred solution salicylaldehyde (IUPAC name: 2-hydroxybenzaldehyde) (10 mmol) in 30 ml of absolute methanol or chloroform in ambient temperature. The color immediately changed to yellow. The mixture was then stirred for 2h in ambient temperature before removal of solvent under vacuum. The result was yellow oil. Yield 86%, Anal. Calc. for $C_{10}H_{11}ON$: C, 74.51; H, 6.88; N, 8.69. Found: C, 74.90; H, 6.76; N, 8.75. FT-IR (KBr, cm^{-1}): (O–H) 3485 (br, vs); (C=N) 1627 (vs). ^{1}HNMR ($CDCl_3$, 400 MHz, 298 K) δppm: 11.1 (1H, s, O*H*); 8.30 (s, 1H, N=C*H*); 7.1- 7.8 (m, 4H, Ar), 6.1 (m, 1H, C*H*=CH_2); 5.3 (d of d, 1H, CH = C*H*H); 5.20 (d of d, 1H, CH=C*H*H), 4.2 (d, CH_2CH=CH_2). ^{13}CNMR ($CDCl_3$, 400 MHz, 298 K) δppm: 166.0, 161.6, 135.3, 132.7, 131.9, 119.5, 119.1, 117.5, 116.9, 61.2.

2.4.Preparation of complexes

2.4.1. General synthesis

A MeOH or $CHCl_3$ solution (20 cm^3) of allylamine (IUPAC name: 3-amino-prop-1-ene) (3 mmol) was added dropwise to a MeOH or $CHCl_3$ solution (20 cm^3) of the salicylaldehyde (IUPAC name: 2-hydroxybenzaldehyde) (3 mmol). The yellow, air stable solution was stirred for 2h in ambient temperature. Then a solution of triethylamine (4 mmol) in absolute MeOH (5 cm^3) was added to the solution. The solution was essentially dark yellow at this time. The mixture stirred for 10 min, and then a solution of appropriate metal salt (1.5 mmol $Zn(NO_3)_2.6H_2O$, $CuCl_2.2H_2O$ and $VO(acac)_2$ salts and 1 mmol for $CoCl_2.6H_2O$ salt) in absolute MeOH (20 cm^3) was added dropwise. The resulting solution was stirred for 12h ambient temperature.

2.4.2. Vanadium (II) complex VOL$_2$

The resultant clear yellow solution was allowed to stand overnight. After concentration at room temperature, dark yellow precipitate was collected by filtration. Appropriate single crystals for X-ray crystallography were obtained directly from the reaction mixture. The typical yield was 72%. Anal. calc. for $C_{20}H_{20}N_2O_3V$: C: 62.02, H: 5.20, N: 7.23. Found: C: 61.87, H: 5.26, N: 7.24. Selected IR data (KBr, cm^{-1}): 1622 ($\nu_{C=N}$), 1473 ($\nu_{C—N}$), 1328 ($\nu_{C—O}$).

2.4.3. Cobalt (II) complex CoL$_3$

The solution was slowly evaporated to dryness at room temperature to yield a red solid which was purified by washing with 50 ml of diethyl ether about five times and the obtained green precipitate was dried in air. The red needle crystals were obtained in chloroform by recrystallization. The typical yield was 79%. Anal. calc. for $C_{30}H_{30}CoN_3O_3$: C: 66.79, H: 5.60, N: 7.79. Found: C: 66.89, H: 5.52, N: 7.90. Selected IR data (KBr, cm^{-1}): 1623 ($\nu_{C=N}$), 1449 ($\nu_{C—N}$), 1322 ($\nu_{C—O}$).

2.4.4. Copper (II) complex CuL$_2$

Dark green crystals were collected by filtration. The green flat crystals were obtained in chloroform by recrystallization. The typical yield was 91%. Anal. calc. for $C_{20}H_{20}CuN_2O_2$: C: 62.57, H: 5.25, N: 7.30. Found: C: 62.70, H: 5.19, N: 7.36. Selected IR data (KBr, cm^{-1}): 1621 ($\nu_{C=N}$), 1472 ($\nu_{C—N}$), 1328 ($\nu_{C—O}$).

2.4.5. *Zinc (II) complex ZnL₂*

The resultant clear yellow solution was allowed to stand overnight. After concentration at room temperature, dark yellow crystals were collected by filtration. Appropriate single crystals for X-ray crystallography were obtained directly from the reaction mixture. The typical yield was 83%. Anal. calc. for $C_{20}H_{20}N_2O_2Zn$: C: 62.27, H: 5.23, N: 7.26. Found: C: 62.43, H: 5.16, N: 7.33. Selected IR data (KBr, cm^{-1}): 1625 ($\nu_{C=N}$), 1433 ($\nu_{C—N}$), 1323 ($\nu_{C—O}$). The ^1H NMR and ^{13}C NMR spectral data are given in Table 1.

3. Results and discussion

The yellow Schiff base **HL**, obtained by the self-condensation reaction between allylamine and salicylaldehyde in absolute methanol or chloroform as solvent at ambient temperature reported in Scheme 1, is a yellow oil, stable in air and moderately soluble in the most common organic solvents. Vanadium(IV), Copper(II) and Zinc(II) Schiff-base complexes where obtained by treating $VO(acac)_2$, $CuCl_2.2H_2O$ and $Zn(NO_3)_2.6H_2O$ with two molar equivalents of the ligand in the presence of triethylamine in room temperature, respectively (Scheme 2). Cobalt(III) Schiff-base complex obtained by adding $CoCl_2.6H_2O$ with three molar equivalents of the ligand in the presence of triethylamine in room tempreture (Scheme 2). All complexes were characterized by elemental analysis (CHN), FT-IR spectroscopy and single crystal X-ray diffraction technique. Also, The Schiff base ligand and its Zinc(II) Schiff base complex were investigated by NMR techniques.

3.1. IR spectra

In the FT-IR spectrum of the ligand, a sharp band appeared at 1627 cm^{-1}, which is attributed to the C=N vibrations of the imine group [35-38]. In the FT-IR spectra of the Schiff base complexes this band appeared at 1622, 1623, 1621 and 1625 cm^{-1} for Vanadium(IV), Cobalt(III), Copper(II) and Zinc(II), respectively [22-30].

The spectrum of free ligand shows strong band in 1328 and 1475 cm^{-1}, assigned to the C—O and C—N stretching of the ligand. However, after complexation of C—O and C—N group via oxygen and nitrogen to the metal ion, these bands were observed at the region of 1329 and 1473 cm^{-1} for Vanadium(IV), 1322 and 1449 cm^{-1} for Cobalt(III), 1328 and 1472 cm^{-1} for Copper(II) and 1323 and 1433 cm^{-1} for Zinc(II) complex. In complexes, absence of the phenolic O—H vibration indicates that ligand is deprotonated in complexes.

Monomeric five coordinated vanadyl complex shows a band around 970 cm^{-1} whereas in polymeric six coordinated vanadyl complexes with linear (polymeric) …V=O…V=O… units this band shifts to lower wave numbers and appears around 860 cm^{-1} [39-42]. Thus the sharp band at 977 cm^{-1} in the FT-IR spectrum of the vanadium(IV) Schiff base complex, **VOL$_2$**, is attributed to V=O vibrations, indicating the monomeric form of the $L_2V=O$ Schiff base complex in the solid state, as confirmed by the single crystal X-ray diffraction.

3.2.NMR spectra

The diamagnetic Zinc(II) complex, **ZnL$_2$**, was studied by ^{1}H and ^{13}C NMR experiments (Table 1). The ^{1}H and ^{13}C NMR were run immediately after solution in $CDCl_3$ and gave the expected simple spectrum, indicating the integrity of the complexes. The spectra obtained after 12, 24 and 120 h were similar to the initial spectra indicating that the complexes are stable in solution.

The ^{1}H NMR spectrum of the complex is almost similar to that of the ligand with slight shift to lower fields. The signal for the imine proton in the zinc complex appears at 8.17 and this is shifted downfield with respect to the corresponding signal in the free ligand, indicating that the metal-nitrogen bond is retained in solution. No signal corresponded to hydroxyl protons at 11.1 ppm, suggested that the hydroxyl groups are fully deprotonated and the oxygen is most likely coordinated to the metal ions. The ^{13}C NMR spectrum shows 10 signals for **ZnL$_2$** complex. The peak at 171.5 ppm, assignable to the imine carbon atoms, confirms the presence of the Schiff base in the complex [35].

3.3.Description of the crystal structures

3.3.1. Structure description of ZnL$_2$

The molecular structure of **ZnL$_2$** is shown in Figure 1. Selected bond distances and angles are listed in Table 3. The molecular structure of the **ZnL$_2$** complex is revealed to be a monomeric complex with an approximately planar configuration about the central zinc centre. The salicylaldiminato ligands are arranged with respect to each other in a *trans* orientation such that one allyl substituent lies above the [CuO2N2] plane and the other below.

The Zn–O distances of 1.8865(17) and 1.8933(18) Å and the Zn–N bond lengths of 1.9999(19) and 2.0111(19) Å are similar to those seen in related complexes [16, 43-45]. For instance, distances of 1.8967(19) and 2.001(2) Å for the Zn–O and Zn–N bonds, respectively, are found in a related bis{2-[(1H-pyrrol-2-yl)methyliminomethyl] phenolato-κ^2N,O}zinc(II) complex derived from (1H-pyrrol-yl)methanamine and salicylaldehyde [45]. The C=C distances in **ZnL$_2$** are 1.295 (4) Å (C9=C10) and 1.293 (4) Å (C19=C20), are well within the range expected for double bonds found in allyl derivatives. The C=N bond distances are 1.288 (3) Å (N1=C7) and 1.285 (3) Å (N2=C17), which are consistent with a slight elongation of the C–N double bond when coordinated to a late metal center [16]. The allyl groups are approximately centrosymmetric to one another but no significant interaction with a metal center is observed, thereby allowing access for covalently bond on an insoluble support as heterogeneous catalysts [18-21].

As we know, non-covalent interactions are at the core of most chemical and biological processes and hence knowledge of their nature, strength, occurrence and consequences is of paramount importance

[46]. The weak non-covalent interactions such as C–H…X (X = O, N, S, halogen) and π-π stacking, while weaker than the classical H-bonds, also play notable roles in conformation, crystal packing, supramolecular assembly and physicochemical properties and thus have implications in drug design, material design and supramolecular synthesis [46–52].

Although there are no classical hydrogen bonds in the structure, but two intramolecular C–H…O contacts are observed in the solid State (Table 4). Intramolecular hydrogen bond occurs between C(8)—H(8B)...O(2) [2.785(3) Å] atoms and C(18)—H(18A)...O(1) [2.771(3) Å] atoms (Fig. 1). The intramolecular C–H…O hydrogen bonds result in the formations of the five membered rings (O2/Zn1/N1/C8/H8B and O1/Zn1/N2/C18/H18A) having envelope conformations with H8B and H18A atoms displaced by 0.605 and 0.606 Å, respectively, from the planes of the other ring atoms.

Another interesting feature of the **ZnL₂** complex, is the presence of π..π and C–H…π interactions (Figures 2 and 3; Tables 5 and 6). C–H…π edge-to-face interactions are present between CH groups with H…π distance of 2.90 Å for C(10)—H(10A)…Cg(4) and 2.95 Å for C(15)—H(15)…Cg(2) [Cg(2) is centroid for C(11)/C(16) ring and Cg(4) is centroid for Zn(1)/O(2)/C(11)/C(16)/C(17)/N(2) ring] (Fig. 2). Also, π..π interactions are exist between Cg(1)…Cg(2) with centroid–centroid distance of 3.7361(15) and 3.8016(15) Å, in which Cg(1) and Cg(2) are centers of Zn(1)/O(1)/C(1)/C(6)/C(7)/N(1) and C(1)/C(6) rings, respectively (Scheme 4, Fig. 3 and Table 6). This continuum of π..π interactions runs parallel to the bc plane.

Reaction of 2-allylsalicylideneimin with $Zn(OAc)_2.2H_2O$ in reflux condition, named **ZSB**, has previously been reported by Johnson *et al* [16]. Single crystal X-ray diffraction studies reveal that this complex to be a dimer with bridging salicylaldiminato ligands resulting in a distorted trigonal bipyramidal geometry around each zinc centre (Scheme 3). Difference in kind of product can be resulted by two reasons: kind of metal ion [($Zn(NO_3)_2.6H_2O$ or $Zn(OAc)_2.2H_2O$)] and reaction condition (reaction under reflux or in room temperature). For investigation of reaction conditions in kind of product (dinuclear or mononuclear complex), we react the Schiff base ligand with $Zn(NO_3)_2.6H_2O$ in reflux condition. The result was mononuclear complex. From this test we understand that change in reaction condition don't change the kind of products. As a result, in comparison with the previously reported zinc dinuclear Schiff-base complex, the formation of the mononuclear zinc complex may be caused only by influence of the used metal ion [$Zn(NO_3)_2.6H_2O$ instead of $Zn(OAc)_2.2H_2O$].

3.3.2. Structure description of VOL$_2$

An ORTEP view of **VOL$_2$** with the atom-numbering scheme is shown in Fig. 4. In this complex, the oxidovanadium(IV) unit is coordinated to two bidentate Schiff base ligands with the two nitrogen and two phenolate oxygen atoms in equatorial positions and one oxygen in the axial position to complete the distorted tetragonal pyramidal N2O3 coordination sphere. The bond angles within the coordination sphere range from 84.57(15)° for O(2)–V(1)–N(1) to 164.03(16)° for O(2)–V(1)–N(2), which indicates a significant distortion of the tetragonal pyramid. The V—O [1.909(3) and 1.899(3) Å] and V—N [2.089(4) and 2.106(4) Å] bond distances in **VOL$_2$** agree well with the same distances and angles in other oxidovanadium(IV) Schiff base complexes [29, 39, 53–57]. The vanadyl (V=O) bond length, 1.583(3) Å, is similar to this bond in other oxidovanadium(IV) Schiff base complexes [29,39,58] and gives a strong absorption in the FT-IR spectrum at 977 cm^{-1}. The two Schiff base ligands coordinate to the vanadium center in a *trans* geometry with respect to each other. As shown in Fig. 4 and Table 4, there are three intramolecular nonclassical C(8)—H(8A)...O(2), C(9)—H(9)...O(3) and C(18)—H(18B)...O(1) hydrogen bonds in **VOL$_2$**. In the molecular packing of **VOL$_2$**, two molecules are connected by intermolecular non-classical C(17)–H(17)…O(3) [2.715(3) Å] hydrogen bonds (Fig. 5). Also, in the lattice, the monomeric **VOL$_2$** moieties are linked to parallel chain through C–H···π stacking interactions (Figure 6). These C–H···π edge-to-face interactions are present between CH group of phenyl rings with Cg(1) with H···π distances of 3.657(6)Å [Cg(1): C(3)—H(3)…Cg(1)]. Additionally, the sum of the weak non-covalent interactions seems to play an important role in the crystal packing and the formation of the framework.

3.3.3. Structure description of CoL$_3$

The molecular structure of **CoL$_3$** is shown in Figure 7. Selected bond distances and angles are listed in Tables 3. The X-ray structural study reveals that the complex crystallizes in the monoclinic system with $P2_1/c$ space group. The coordination sphere about cobalt consists of three phenolato oxygens and three imino nitrogen atoms from three Schiff base ligands, then the cobalt(III) ion adopts a distorted octahedral geometry. Each Schiff base ligand acts as a chelate using a phenolato oxygen and an imino nitrogen. In this complex, the equatorial plane is formed by the coordination of three imino nitrogen atoms [N(1), N(2) and N(3)] from three Schiff base ligands and one phenolato oxygen atom [O(1)] from one Schiff base ligand. The apical positions are occupied by two phenolic oxygen atoms [O(2) and O(3)] from two Schiff base ligands. Average bond length of Co—N (~1.94 Å) is slightly longer than the average bond length of Co—O (~1.90 Å). The average bond angles of *cis*-N-Co-O, *cis*-O-Co-O and *cis*-N-Co-N angles and the bond angles of *trans*-N-Co-O, *trans*-O-Co-O and *trans*-N-Co-N angles are similar to those reported for Co(III) complex derived from 5-bromo-2-hydroxybenzyl-2-furylmethyl)-imine as bidentate schiff base ligand (Table 3) [59].

As depicted in Fig. 8, in the crystal packing of **CoL$_3$**, adjacent molecules are assembled through week C—H…π stacking interaction. These C–H···π stacking interactions are present between CH groups and aromatic rings with H···π distances of 2.93 Å and 2.97 Å for C(2)—H(2)…Cg(5) and C(17)—H(17)…Cg(6), respectively, in which Cg(5) is the centroid for the C(11)/C(16) ring and Cg(6) is the centroid for the C(21)/C(26) ring (Fig. 8 and Table 5). These C–H···π interactions form a layer structure along the crystallographic bc plane [011].

3.3.4. Structure description of CuL_2

CuL_2 complex has previously been synthesized in reflux condition by Johnson *et al* with copper acetate as metal ion and the molecular structure of that has been described [16]. As part of this study, we synthesized this complex again in room temperature with copper chloride dihydrate for understanding the effect of these two elements (kind of metal ion and reaction condition) in kind of product. As we said about zinc complex in above, we can go from binuclear zinc(II) complex to mononuclear zinc(II) complex with change of metal ion [$Zn(OAc)_2.2H_2O$ instead of $Zn(NO_3)_2.6H_2O$]. However, for Cu(II) complex, different metal ions and different reaction condition don't have any influence on the product and the products in different conditions are identical.

An ORTEP view of **CuL_2** with the atom-numbering scheme is presented in Fig. 9 and the crystallographic data and selected bond lengths and angles are collected in Tables 2 and 3. The crystallographic data reveal that the metal center are four-coordinated by two phenolate oxygen and two imine nitrogen atoms of two Schiff base ligands. The ligands coordinate to the Cu(II) center in *trans* geometry with respect to each other. The geometry around the metal center is a distorted square-planar, with $P2_1/c$ space group, as indicated by the unequal metal–ligand bond distances and angles. Similar to **ZnL_2** complex, two non-classical intramolecular hydrogen bonds of the type C—H…O are formed between the C—H in the CH_2 group as donors and O in the salicylal moiety as acceptors (Fig. 9, Table 4). Similar to **ZnL_2** complex, there are two intermolecular C–H…π interactions in **CuL_2** complex (Figures 10 and 11; Tables 5 and 6). C–H…πedge-to-face interactions are present between CH groups with H…πdistance of 2.98 Å for C(5)—H(5)…Cg(1) and 2.90 Å for C(20)—H(20)…Cg(3)

[Cg(1) is centroid for Cu(1)/O(1)/C(1)/C(6)/C(7)/N(1) ring and Cg(3) is centroid for C(1)/C(6) ring] (Fig. 10).

As depicted in Fig. 11, in the crystal packing of **CuL_2**, adjacent molecules are assembled through π–π stacking interaction and extended along b-axis. Centroid–centroid distances between two rings are 3.748(2) and 3.803(2) Å, a typical distance for systems held by π..πstacking interactions [60].

4. Conclusion

In conclusion, we have synthesized four macroacyclic Schiff base V(IV), Co(III), Cu(II) and Zn(II) complexes derived from an asymmetric bidentate Schiff-base ligand (**HL**) at ambient temperature. Ligand and all complexes were characterized by the elemental analysis (CHN) and FT-IR spectroscopy. Also, ^{1}H and ^{13}C NMR techniques were employed for characterization of the ligand (**HL)** and diamagnetic complex **ZnL_2**. The structures of all complexes have been established by using single crystal X-ray diffraction analysis. The Zn(II) and Cu(II) atoms are coordinated by two phenolic-O atoms and two azomethine-N atoms to form a square-planar geometry. In the structure of Co(III) complex, the coordination sphere about Cobalt(III) consists of three phenolato oxygens and three imino nitrogen atoms from three Schiff base ligands, then the cobalt(III) ion adopts a distorted octahedral geometry. The Vanadium(IV) complex crystallizes in the monoclinic system, with space group $P2_1/c$, having one symmetry-independent V^{4+} ion coordinating in an approximately square pyramidal N_2O_3 geometry by two imine nitrogen, two phenolato oxygen atoms from two Schiff base ligands in a square plane and one oxygen atom in an apical position.

Acknowledgement

The authors are grateful to the Research Council of the University of Isfahan for financial support of this work.

Appendix A. Supplementary data

Crystallographic data for the structures in this paper have been deposited with the Cambridge Crystallographic Data Centre as the supplementary publication no. CCDC 1021989, 1021987, 1021988 and 1021986 for **ZnL_2**, **CuL_2**, **VOL_2** and **CoL_3**, respectively. Copies of the data can be obtained, free of charge, on application to CCDC, 12 Union Road, Cambridge CB21EZ, UK (Fax: +44 1223 336033 or e-mail: deposit@ccdc.cam.ac.uk).

References

[1] S. Yamada, Coord. Chem. Rev. 190–192 (1999) 537.

[2] R.H. Holm, J. Am. Chem. Soc. 82 (1960) 5632.

[3] A.D. Garnovskii, A.P. Sadimenko, M.I. Sadimenko, D.A. Garnovskii, Coord. Chem. Rev. 173 (1998) 31.

[4] S.D. Bella, G. Consiglio, S. Sortino, G. Giancane, L. Valli, Eur. J. Inorg. Chem. 33 (2008) 5228.

[5] Ch. T. Lyons , T. D. P. Stack, Coord. Chem. Rev., 257 (2) (2013) 528.

[6] P. G. Cozzi, Chem. Soc. Rev., 33 (2004) 410.

[7] K.C. Gupta, A. K. Sutar, Coord. Chem. Rev., 252 (1) (2013) 1420.

[8] S. Sarkar, S. Biswas, M.-S. Liao, T. Kar, Y. Aydogdu, F. Dagdelen, G. Mostafa, A. P. Chattopadhyay, G. P.A. Yap, R-H. Xie, A. T. Khan, K. Dey, Polyhedron 27 (16) (2008) 3359.

[9] G. Barone, A. Terenzi, A. Lauria, A. M. Almerico, J. M. Leal, N. Busto, B. García, Coord. Chem. Rev., 257 (19) (2013) 2848.

[10] J. Lu, J. Ju, X. Bo, H. Wang, L. Guo, Electroanalysis, 25 (2013) 2531.

[11] L. Mao, K. Yamamoto, W. Zhou, L. Jin, Electroanalysis 12 (2000) 72.

[12] P. Noblia, M. Vieites, B.S. Parajon-Costa, E.J. Baran, H. Cerecetto, P. Draper, M. Gonzalez, O.E. Piro, E.E. Castellano, A. Azqueta, A.L. Cerain, A. Monge-Vega, D. Gambino, J. Inorg. Biochem. 99 (2005) 443.

[13] Ö. Güngör, P. Gürkan, J. Mol. Struct. 1074 (2014) 62.

[14] L.A. Saghatforoush, F. Chalabian, A. Aminkhani, G. Karimnezhad, S. Ershad, Eur. J. Med. Chem., 44 (2009) 4490.

[15] K. Singh, M. S. Barwa, P. Tyagi, Eur. J. Med. Chem., 41 (2006) 147.

[16] N. Poulter, M. Donaldson, G. Mulley, L. Duque, N. Waterfield, A. G. Shard, S. Spencer, A. Tobias, A. Jenkins, A. L. Johnson, New. J. Chem., 35 (2011) 1477.

[17] S. Majumder, A. Bhattacharya, J. P. Naskar, P. Mitra, S. Chowdhury, Inorg. Chim. Acta, 399 (2013) 166.

[18] B. Carlos, G. Bárbara, G. Hermenegildo, C. Avelino. J. Catalysis. 215 (2003) 199.

[19] B. Carlos, G. Bárbara, G. Hermenegildo, C. Avelino. J. Catalysis. 221 (2004) 77.

[20] B. Carlos, G. Bárbara, G. Hermenegildo, C. Avelino. Tetrahedron 60 (2004) 10461.

[21] B. Carlos, G. Bárbara, G. Hermenegildo, C. Avelino. Tetrahedron Lett. 44 (2003) 6813.

[22] G. Grivani, V. Tahmasebi, K. Eskandari, A. Dehno Khalaji, G. Bruno, H. Amiri Rudbari, J. Mol. Struct. 1054 (2013) 100.

[23] H. Iranmanesh, M. Behzad, G. Bruno, H. Amiri Rudbari, H. Nazari, A. Mohammadi, O. Taheri, Inorg. Chim. Acta, 395 (2013) 81.

[24] M. Pooyan, A. Ghaffari, M. Behzad, H. Amiri Rudbari, G. Bruno, J. Coord. Chem. 66 (2013) 4255.

[25] A, Ghaffari, M. Behzad, M. Pooyan, H. Amiri Rudbari, G. Bruno, J. Mol. Struct. 1063 (2014) 1.

[26] H. Iranmanesh, M. Behzad, G. Bruno, H. Amiri Rudbari, H. Nazari, A. Mohammadi, O. Taheri, Inorg. Chim. Acta 395 (2013) 81.

[27] H. Keypour, M. Shayesteh, D. Nematollahi, L. Valencia, H. Amiri Rudbari, J. Coord. Chem. 63 (23) (2010) 165.

[28] G. Grivani, M. Vakili, A. D. Khalaji, G. Bruno, H. Amiri Rudbari, M. Taghavi, V. Tahmasebi, J. Mol. Struct. 1072 (2014) 77.

[29] G. Grivani, G. Bruno, H. Amiri, A.D. Khalaji, P. Pourteimouri, Inorg. Chem. Commun. 18 (2012) 15.

[30] H. Keypour, R. Azadbakht, H. Amiri Rudbari, A. Heydarinekoo, H. R Khavasi, Transition Met. Chem., 34 (2009) 835.

[31] X-AREA, version 1.30, program for the acquisition and analysis of data, Stoe & Cie GmbH, Darmstadt, Germany, 2005.

[32] (a) X-RED, version 1.28b, program for data reduction and absorption correction, Stoe & Cie GmbH, Darmstadt, Germany, 2005; (b) X-SHAPE, version 2.05, program for crystal optimization for numerical absorption correction, Stoe & Cie GmbH, Darmstadt, Germany, 2004.

[33] M.C. Burla, R. Caliandro, M. Camalli, B. Carrozzini, G.L. Cascarano, L. De Caro, C. Giacovazzo, G. Polidori, R. Spagna, J. Appl. Crystallogr. 38 (2005) 381.

[34] G.M. Sheldrick, SHELXL97, University of Göttingen, Göttingen, Germany, 1997.

[35] H. Keypour, H. Amiri Rudbari, R. Azadbakht, E. Abouzari Lotf, J. Chem. Res. (2009) 361.

[36] H. Amiri Rudbari, A. Varasteh Moradi, Synthesis (2010) 205.

[37] H. Keypour, H. Amiri Rudbari, R. Azadbakht. Synth. Commun. 40 (2010) 1486.

[38] H. Amiri Rudbari, A. Varasteh Moradi, R. Azadbakht. Synth. Commun. 41 (2011) 528.

[39] G. Grivani, V. Tahmasebi, A. D. Khalaji, Polyhedron. 68 (2014) 144.

[40] R. Ando, S. Mori, M. Hayashi, T. Yagyu, M. Maeda, Inorg. Chim. Acta 357 (2004) 1177.

[41] R. Ando, H. Ono, T. Yagyu, M. Maeda, Inorg. Chim. Acta 357 (2004) 817.

[42] C.J. Chang, J.A. Labinger, H.B. Gray, Inorg. Chem. 36 (1997) 5927.

[43] D. Zhang, H. Yu, Y-B. Jin, K-W. Lei, Acta Cryst. E68 (2012) m1424.

[44] Y-J. Cai, P. Huang, J. Li, Q. Wang, Acta Cryst. E65 (2009) m1115.

[45] Y-M. Cui, X. Zhang, L. Liu, Q. Wang, Acta Cryst. E65 (2009) m1151.

[46] K. M. Sureshan, T. Uchimaru, Y. Yao and Y. Watanabe, CrystEng-Comm, 2008, 10, 493.

[47] S. Sharma and T. P. Radhakrishnan, J. Phys. Chem. B, 2003, 107, 147.

[48] A. Kanazawa, T. Ikeda and J. Abe, J. Am. Chem. Soc., 2001, 123,1748.

[49] C. Q. Wan, X. D. Chen and T. C. W. Mak, CrystEngComm, 2008, 10,475.

[50] X. P. Zhou, X. Zhang, S. H. Lin and D. Li, Cryst. Growth Des., 2007,7, 487.

[51] D. QuiEonero, C. Garau, C. Rotger, A. Frontera, P. Ballester, A. Costa and P. M. Dey, Angew. Chem., Int. Ed., 2002, 41, 3389.

[52] P. D. Hoog, P. Gamez, I. Mutikainen, U. Turpeinen and J. Reedijk, Angew. Chem., Int. Ed., 2004, 43, 5815.

[53] S. Rayati, N. Torabi, A. Ghaemi, S. Mohebbi, A. Wojtczak, A. Kozakiewicz, Inorg. Chim. Acta 361 (2008) 1239.

[54] K. Fujiwara, T. Ishida, Polyhedron 30 (2011) 3073.

[55] J. Rahchamani, M. Behzad, A. Bezaatpour, V. Jahed, G. Dutkiewicz, M. Kubicki, M. Salehi, Polyhedron 30 (2011) 2611.

[56] M.P. Weberski, C.C. McLauchlan, C.G. Hamaker, Polyhedron 25 (2006) 119.

[57] S. Rayati, M. Koliaei, F. Ashouri, S. Mohebbi, A. Wojtczak, A. Kozakiewicz, Appl. Catal. A 346 (2008) 65.

[58] G. Grivani, S. Delkhosh, K. Fejfarová, M. Dušek, A. D. Khalaji, Inorg. Chem. Commun. 27 (2013) 82.

[59] A.D. Khalaji, S. Maghsodlou Rad, G. Grivani, M. Rezaei, K. Gotoh, H. Ishida, Chin. J. Chem. 29 (2011) 1613.

[60] (a) C. Janiak, J. Chem. Soc. Dalton Trans. (2000) 3885; (b) C.A. Hunter, J.K. Sanders, J. Am. Chem. Soc. 112 (1990) 5525; (c) C.A. Hunter, K.R. Lawson, J. Perkins, C.J. Urch, J. Chem. Soc. Perkin Trans. 2 (2001) 651.

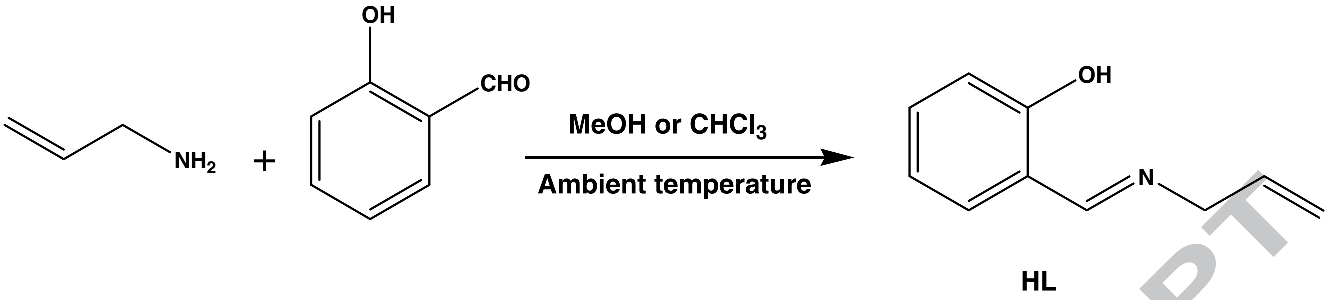

Scheme 1. Synthesis of ligand (**HL**)

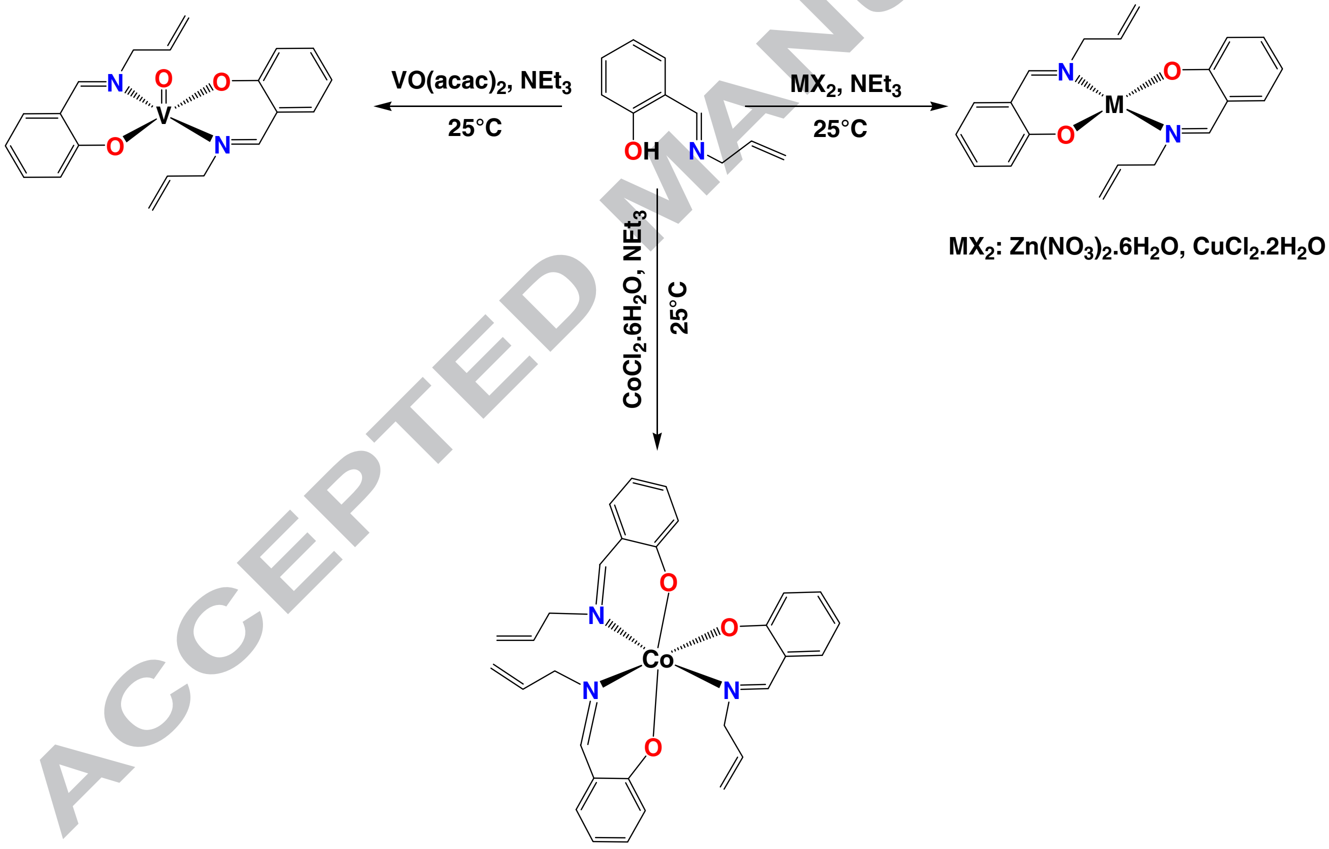

Scheme 2. Synthetic routes for the preparation of the complexes

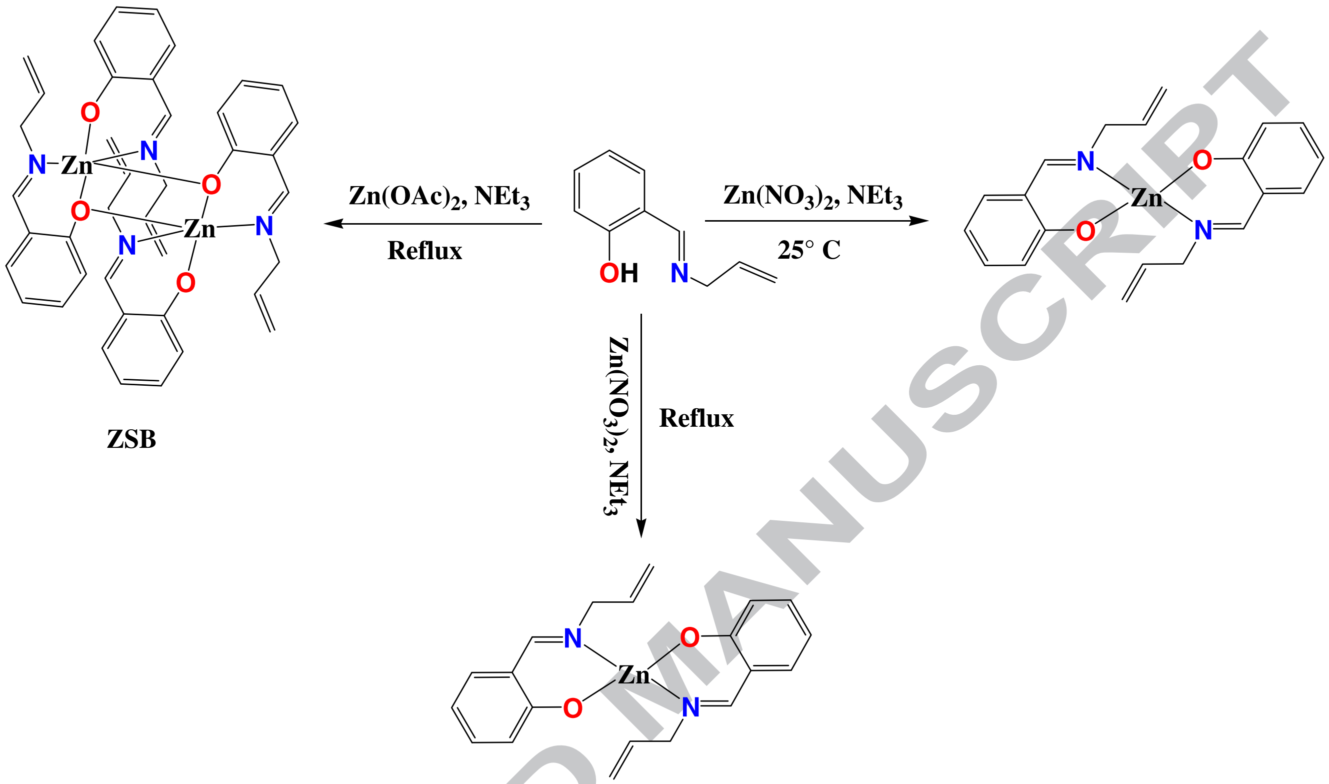

Scheme 3. Simplified scheme showing synthesis of the Zinc(II) Schiff-base complexes with $Zn(OAc)_2$ in reflux condition [16] and with $Zn(NO_3)_2$ in reflux condition and ambient temperature.

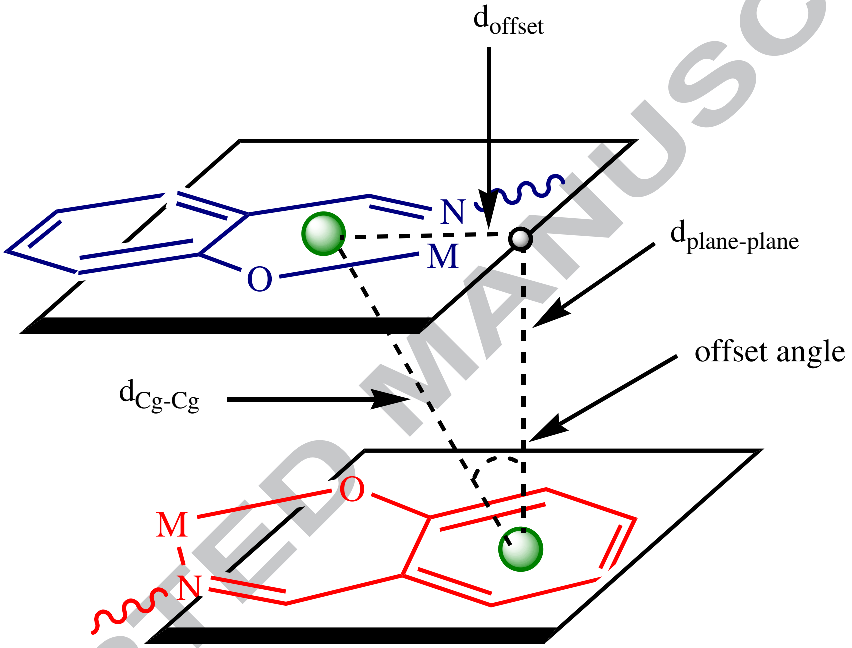

Scheme 4 Schematic representation of geometrical parameters for definition of π–π stacking between two rings (M= Zn(II) and Cu(II).

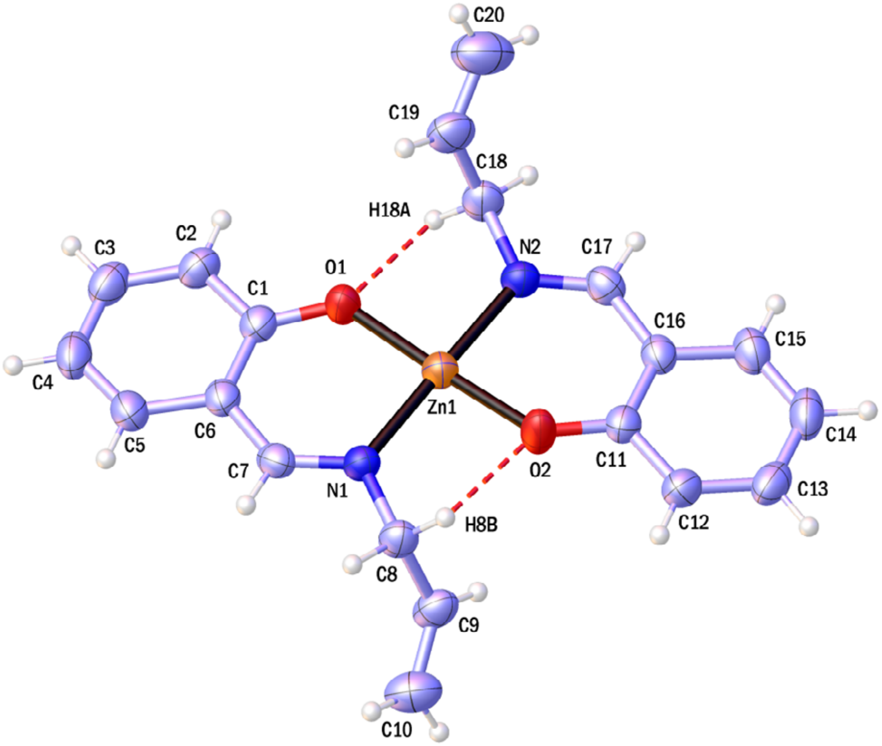

Fig. 1. ORTEP representation of **ZnL_2**. Displacement ellipsoids are drawn at the 50% probability level and H atoms are shown as small spheres of arbitrary radii. Hydrogen bonds are shown as dashed lines.

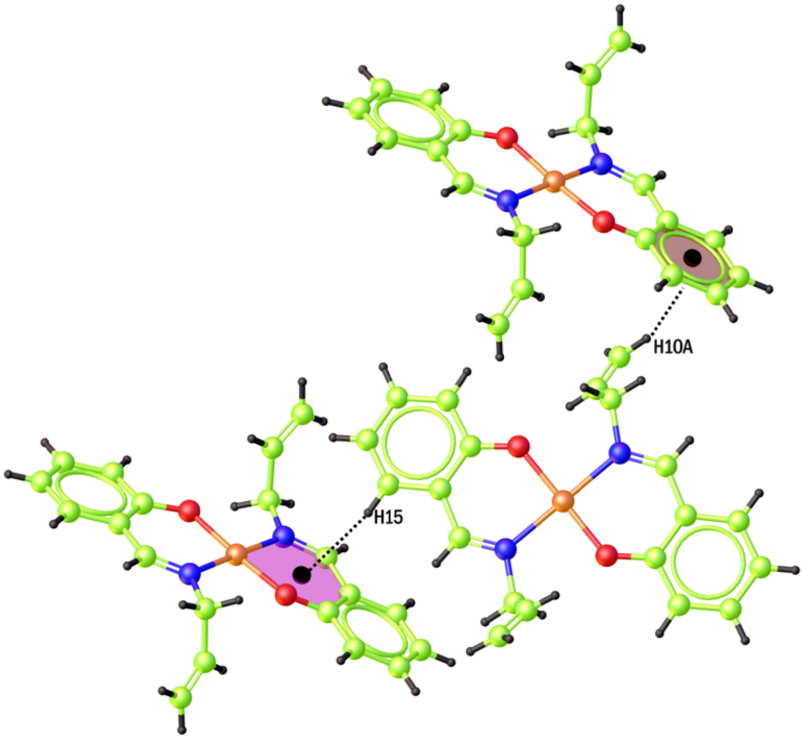

Fig. 2. Illustration of C—H…πinteractions in molecular structure of **ZnL$_2$**

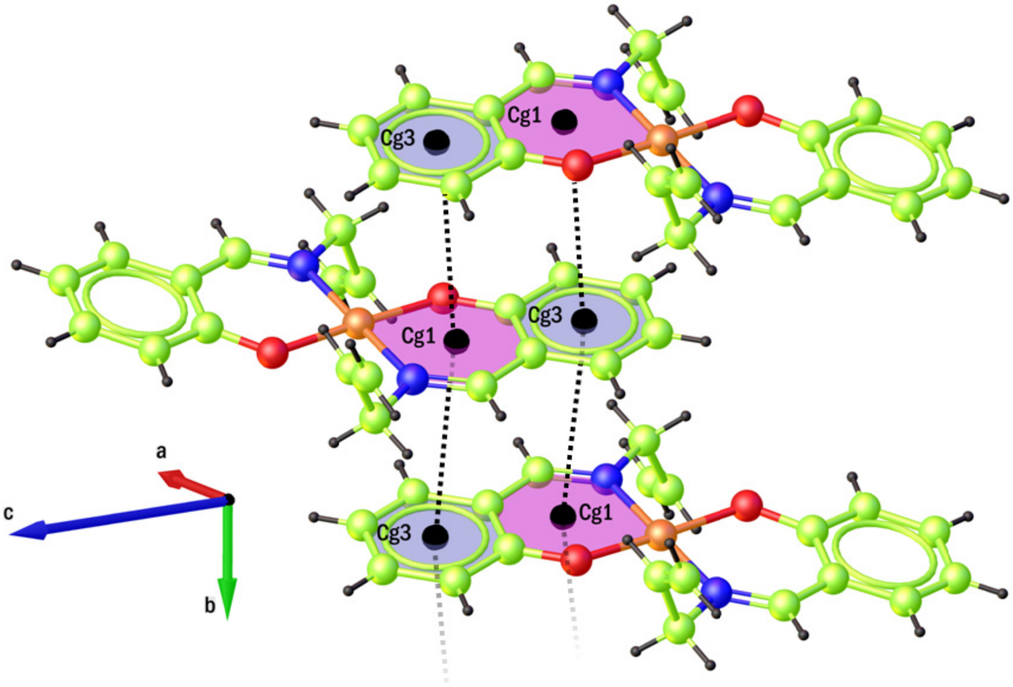

Fig. 3. A side view representation of **ZnL$_2$** showing intermolecular π…π stacking interaction between *Cg*1—*Cg*2 with centroid–centroid distance of 3.736(15) Å and 3.8016(15) Å.

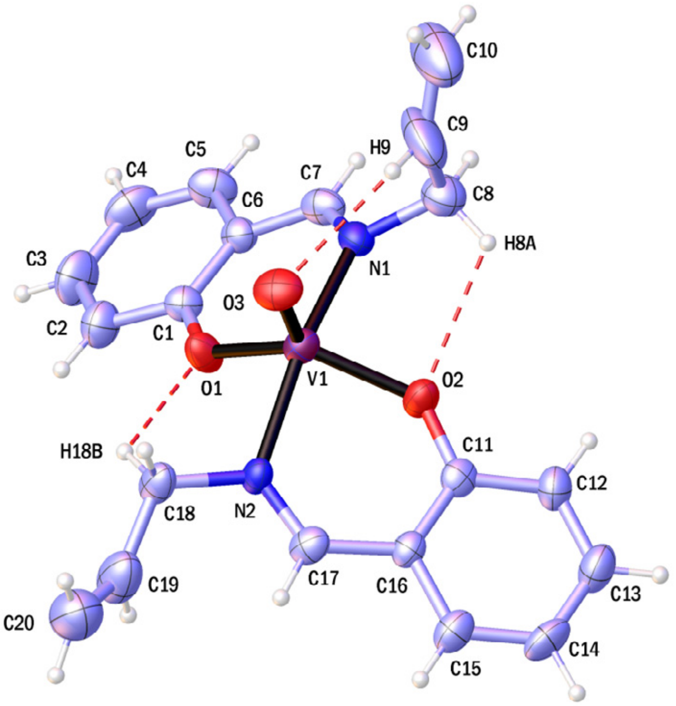

Fig. 4. ORTEP representation of **VOL$_2$**. Displacement ellipsoids are drawn at the 50% probability level and H atoms are shown as small spheres of arbitrary radii. Hydrogen bonds are shown as dashed lines.

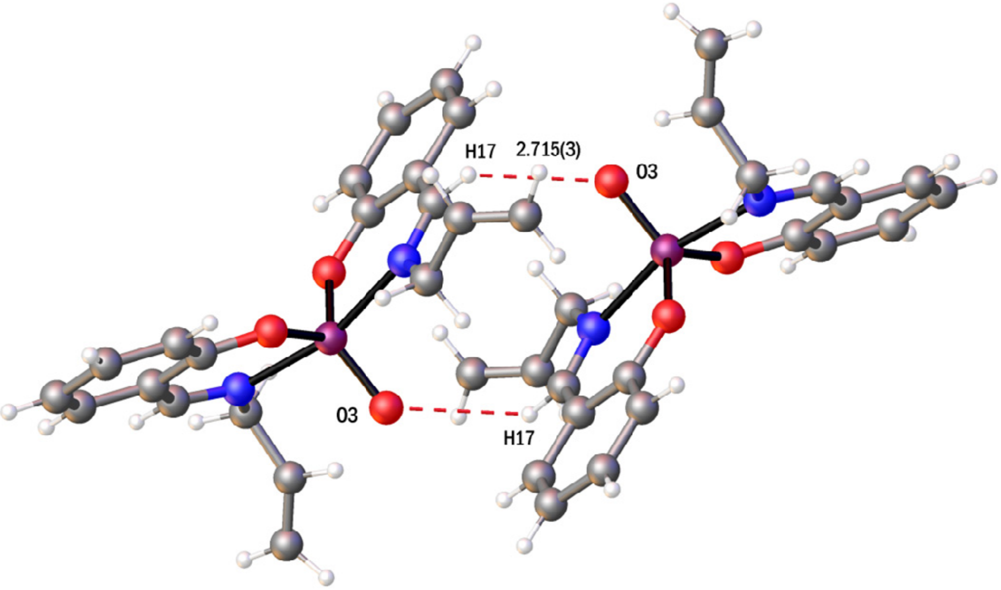

Fig. 5. Crystal packing of **VOL$_2$**. Dashed lines represent the nonclassical hydrogen bonds

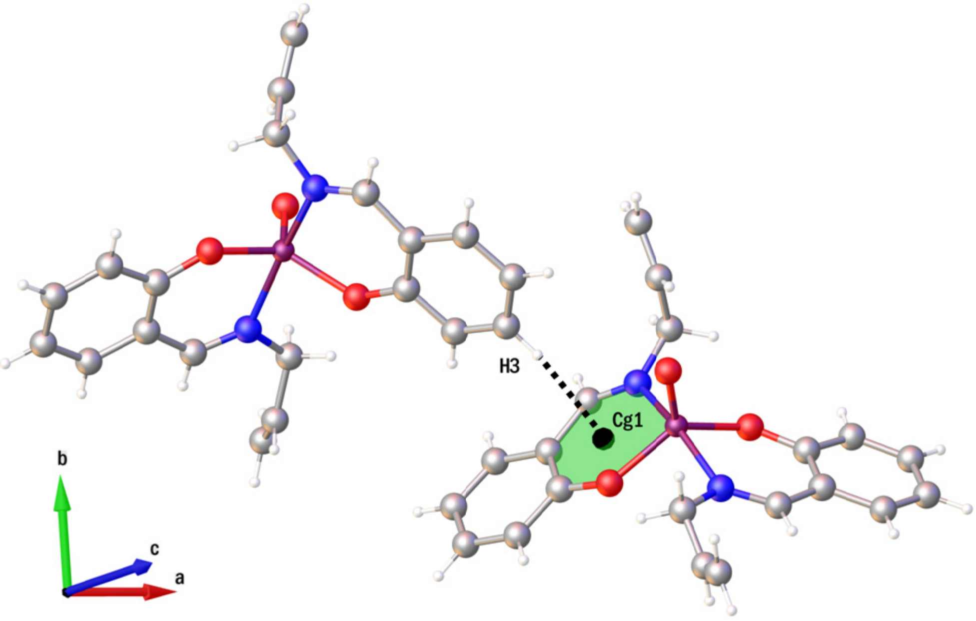

Fig. 6. Illustration of C—H…π interactions in molecular structure of **VOL$_2$**

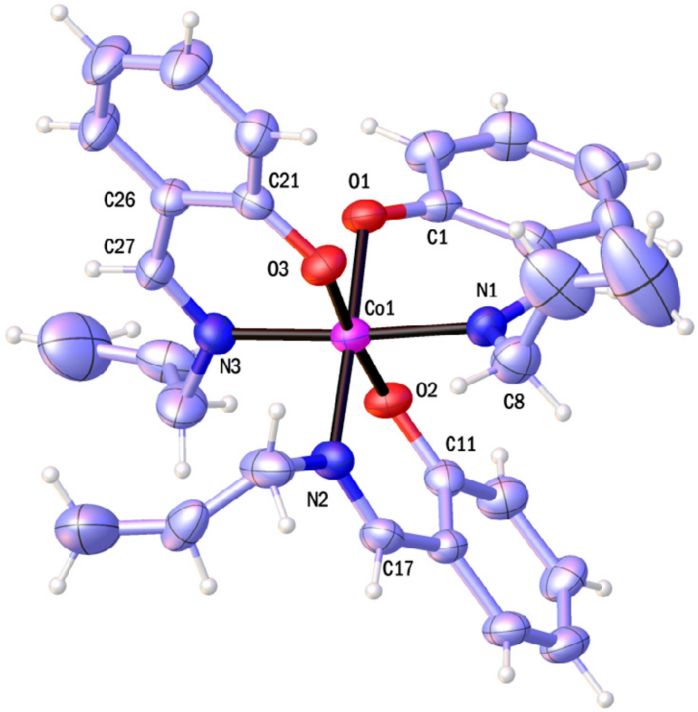

Fig. 7. ORTEP representation of **CoL_3**. Displacement ellipsoids are drawn at the 50% probability level and H atoms are shown as small spheres of arbitrary radii.

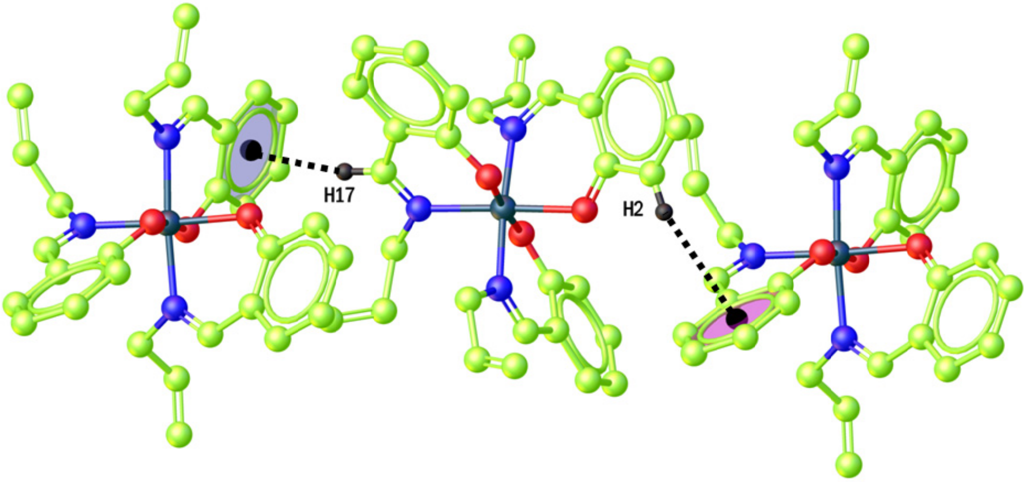

Fig. 8. Illustration of C—H…πinteractions in molecular structure of **CoL_3**

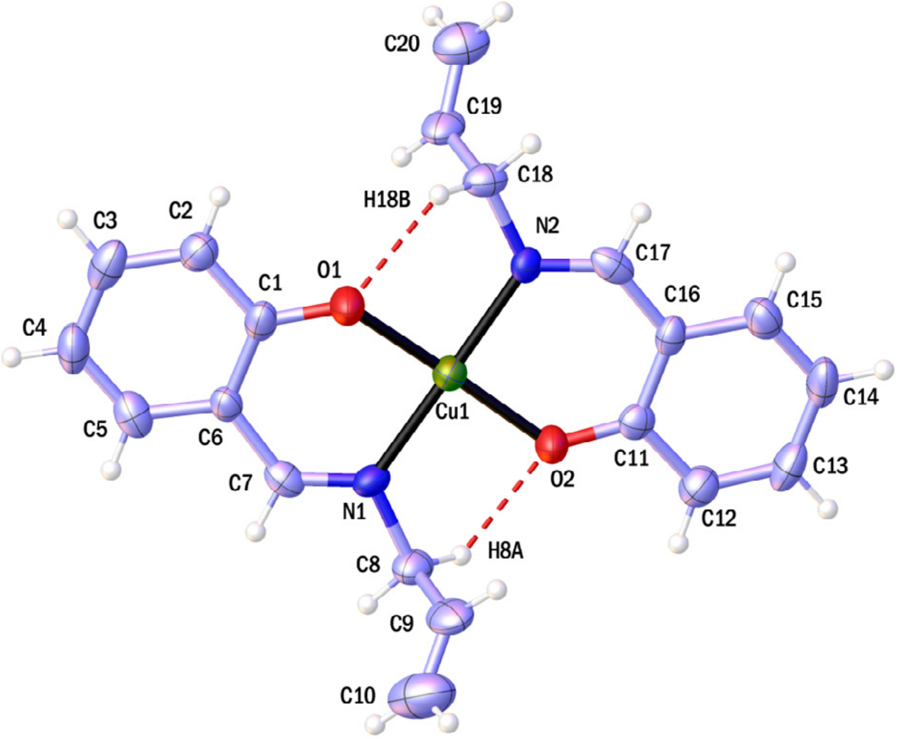

Fig. 9. ORTEP representation of **CuL$_2$**. Displacement ellipsoids are drawn at the 50% probability level and H atoms are shown as small spheres of arbitrary radii. Hydrogen bonds are shown as dashed lines.

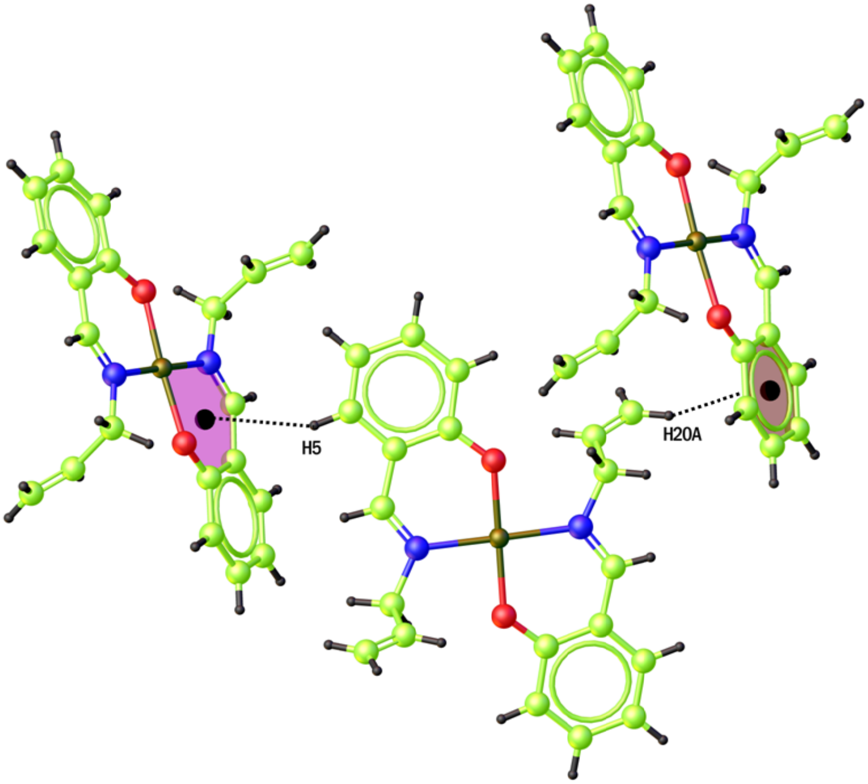

Fig. 10. Illustration of C—H…πinteractions in molecular structure of **CuL$_2$**

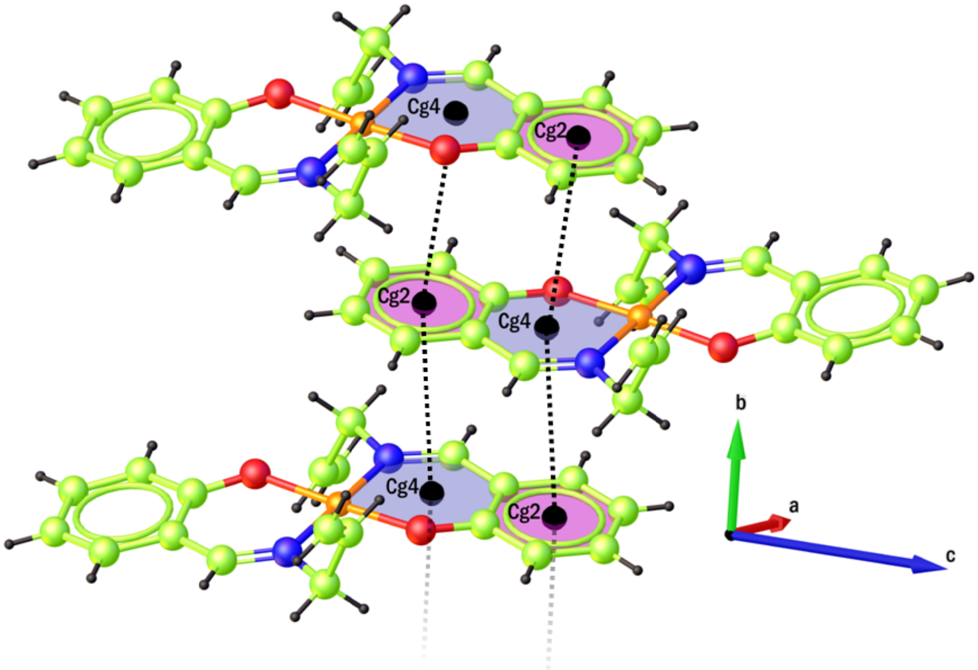

Fig. 11. A side view representation of **CuL_2** showing intermolecular π…π stacking interaction between *Cg*2—*Cg*4 with centroid–centroid distance of 3.748(2) Å and 3.803(2) Å.

Table 1. ^{1}H NMR and ^{13}C NMR data for **ZnL$_2$** complex

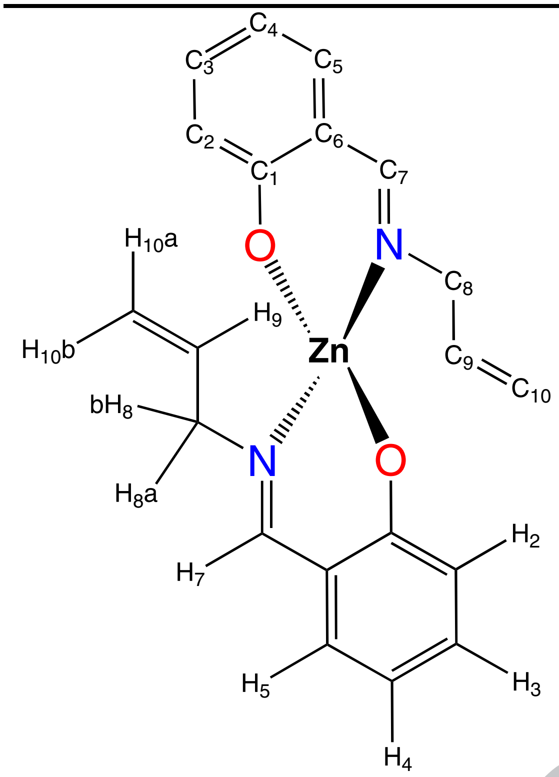

^{1}HNMR		^{13}CNMR	
H_7	8.17(s)	C_7	171.5
H_3	7.32(t)	C_1	165.7
H_5	7.26(d of d)	C_3	135.1
H_2	6.86(d)	C_9	135.8
H_4	6.62(t)	C_5	133.2
H_9	5.85 (m)	C_4	123.1
H_{10b}	5.20(d)	C_2	119.6
H_{10a}	5.08(d)	C_6	118.5
H_{8a},H_{8b}	4.32(d)	C_{10}	114.5
		C_8	62.8

s, singlet; d, doublet; t, triplet; m, multiplet

Table 2 Crystal data and structure refinement.

	ZnL$_2$	**VOL$_2$**	**CoL$_3$**	**CuL$_2$**
Empirical formula	$C_{20}H_{20}N_2O_2Zn$	$C_{20}H_{20}N_2O_3V$	$C_{30}H_{30}N_3O_3Co$	$C_{20}H_{20}N_2O_2Cu$
Formula weight	385.75	387.32	539.50	383.92
Temperature	298(2) K	298(2) K	298(2) K	298(2) K
Wavelength	0.71073 Å	0.71073 Å	0.71073 Å	0.71073 Å
Crystal system	Monoclinic	Monoclinic	Monoclinic	Monoclinic
Space group	$P2_1/c$	$P2_1/c$	$P2_1/c$	$P2_1/c$
Unit cell dimensions	a = 10.780(2) Å b = 7.4988(15) Å c = 22.375(5) Å β = 103.04(3)°	a = 9.808(2) Å b = 8.8710(18) Å c = 22.065(4) Å β = 99.64(3)°	a = 9.2121(18) Å b = 19.438(4) Å c = 15.275(3) Å β = 96.14(3)	a = 10.795(2) Å b = 7.5114(15) Å c = 22.420(5)Å β = 102.91(3)
Volume	1762.1(6) Å^3	1892.6(7) Å^3	2719.6(9) Å^3	1772.0(6) Å^3
Z	4	4	4	4
Density (calculated)	1.454 Mg/m^3	1.359 Mg/m^3	1.318 Mg/m^3	1.439 Mg/m^3
Absorption coefficient	1.409 mm^{-1}	0.545 mm^{-1}	0.666 mm^{-1}	1.248 mm^{-1}
F(000)	800	804	1128	796
Theta range for data collection	2.87 to 25.00°	2.48 to 25.00°	2.49 to 25.00°	2.97 to 25.00°
Index ranges	$-12 \leq h \leq 12$ $0 \leq k \leq 8$ $0 \leq l \leq 26$	$-11 \leq h \leq 11$ $-10 \leq k \leq 10$ $-26 \leq l \leq 24$	$-10 \leq h \leq 10$ $-23 \leq k \leq 0$ $-18 \leq l \leq 18$	$-12 \leq h \leq 12$ $-8 \leq k \leq 8$ $-26 \leq l \leq 26$
Reflections collected	3095	11041	8830	9898
Independent reflections	3095 [$R_{(int)}$ = 0.0408]	3335 [$R_{(int)}$ = 0.1060]	4780 [$R_{(int)}$ = 0.0725]	3108 [$R_{(int)}$ = 0.0798]
Data Completeness	99.8 %	99.9 %	99.9 %	99.8 %
Refinement method	Full-matrix least-squares on F^2	Full-matrix least-squares on F^2	Full-matrix least-squares on F^2	Full-matrix least-squares on F^2
Data / restraints / parameters	3095 / 0 / 226	3335 / 3 / 235	4780 / 8 / 363	3108 / 0 / 226
Goodness-of-fit on F^2	0.937	0.877	0.969	0.954
Final R indices [$I>2\sigma(I)$]	R_1 = 0.0287 wR_2 = 0.0776	R_1 = 0.0418 wR_2 = 0.0708	R_1 = 0.0369 wR_2 = 0.0567	R_1 = 0.0312 wR_2 = 0.0355
R indices (all data)	R_1 = 0.0363 wR_2 = 0.0788	R_1 = 0.1512 wR_2 = 0.0829	R_1 = 0.1496 wR_2 = 0.0652	R_1 = 0.1015 wR_2 = 0.0426
Largest diff. peak and hole	0.200 and -0.490 e.Å^{-3}	0.418 and -0.237 e.Å^{-3}	0.209 and -0.284 e.Å^{-3}	0.237 and -0.328 e.Å^{-3}

Table 3. Selected bond distances (Å) and angles (°) for **ZnL$_2$**, **VOL$_2$**, **NiL$_2$** and **CoL$_3$**.

	ZnL$_2$	**VOL$_2$**	**CuL$_2$**	**CoL$_3$**
M(1)*—O(1)	1.8865(17)	1.909(3)	1.902(2)	1.905(3)
M(1)—O(2)	1.8933(18)	1.899(3)	1.896(2)	1.893(3)
M(1)—N(1)	1.9999(19)	2.089(4)	2.014(3)	1.935(3)
M(1)—N(2)	2.0111(19)	2.106(4)	2.003(3)	1.944(3)
M(1)—O(3)		1.583(3)		1.910(3)
M(1)—N(3)				1.947(3)
O(1)-M(1)-O(2)	176.49(9)	127.30(16)	176.45(14)	86.56(12)
O(1)-M(1)-N(1)	92.62(8)	87.22(16)	91.11(13)	89.99(15)
O(2)-M(1)-N(1)	88.17(8)	84.57(15)	88.14(13)	90.47(15)
O(1)-M(1)-N(2)	88.04(8)	87.11(14)	88.44(12)	176.18(15)
O(2)-M(1)-N(2)	91.23(8)	164.03(16)	92.38(12)	90.82(14)
N(1)-M(1)-N(2)	178.63(8)	164.03(16)	178.61(13)	92.82(17)
C(1)-O(1)-M(1)	129.78(15)	133.5(3)	130.3(3)	118.9(3)
C(17)-N(2)-M(1)	123.98(16)	126.3(3)	122.9(3)	121.4(3)
C(18)-N(2)-M(1)	120.67(15)	115.0(3)	120.6(2)	120.8(3)
C(11)-O(2)-M(1)	130.04(16)	134.3(3)	130.1(2)	121.3(3)
C(7)-N(1)-M(1)	123.24(16)	126.5(4)	123.9(3)	122.0(3)
C(8)-N(1)-M(1)	121.46(14)	118.1(3)	120.2(3)	119.7(3)
O(2)-M(1)-O(3)				175.31(13)
O(1)-M(1)-O(3)				91.29(12)
O(3)-M(1)-N(1)				85.35(15)
O(2)-M(1)-N(2)				90.82(14)
O(3)-M(1)-N(2)				91.52(15)
O(1)-M(1)-N(3)				86.10(14)
O(3)-M(1)-N(3)				93.20(15)
N(1)-M(1)-N(3)				175.81(16)
N(2)-M(1)-N(3)				91.15(16)
C(21)-O(3)-M(1)				122.7(3)
C(27)-N(3)-M(1)				121.7(3)
C(28)-N(3)-M(1)				119.4(3)

* M= Zn for **ZnL$_2$**, V for **VOL$_2$**, Ni for NiL$_2$, Co in case of **CoL$_3$**

Table 4. Intramolecular hydrogen bond geometries (Å,°) for **ZnL_2, CuL_2** and **VOL_2**

	D—H...A	**D—H**	**H...A**	**D...A**	**D—H...A**
ZnL_2					
	C(8)—H(8B)...O(2)	0.97	2.38	2.785(3)	104
	C(18)—H(18A)...O(1)	0.97	2.37	2.771(3)	104
CuL_2					
	C(8)—H(8A)...O(2)	0.97	2.35	2.766(5)	105
	C(18)—H(18B)...O(1)	0.97	2.35	2.777(5)	106
VOL_2					
	C(8)—H(8A)...O(2)	0.97	2.47	3.009(7)	115
	C(9)—H(9)...O(3)	0.93	2.40	3.179(8)	141
	C(18)—H(18B)...O(1)	0.97	2.40	3.012(7)	121

Table 5 Analysis of X—H…Cg(Pi-Ring) Interactions (H…Cg < 3.0 Ang) for **ZnL_2, CuL_2, VOL_2** and **CoL_3**

X—H(I)…Cg(J)*	H…Cg	X…Cg	X—H…Cg
ZnL_2			
C(10)—H(10A) …Cg(4)	2.90	3.760(3)	154
C(15)—H(15)…Cg(2)	2.95	3.717(3)	140
CuL_2			
C(5)—H(5)…Cg(1)	2.98	3.735(4)	140
C(20)—H(20A)…Cg(3)	2.90	3.768(5)	156
VOL_2			
C(3) —H(3)…Cg(1)	2.84	3.657(6)	147
CoL_3			
C(2)—H(2)…Cg(5)	2.93	3.815(6)	159
C(17)—H(17)…Cg(6)	2.97	3.825(5)	154

* For **ZnL_2** Cg(4): C(11)/C(16) ring; Cg(2): Zn(1)/O(2)/C(11)/C(16)/C(17)/N(2) ring; for **CuL_2** Cg(1): Cu(1)/O(1)/C(1)/C(6)/C(7)/N(1) ring; Cg(3): C(1)/C(6) ring. For **VOL_2** Cg(1): V(1)/O(1)/C(1)/C(6)/C(7)/N(1); For **CoL_3** Cg(5): C(11) /C(16) ring; Cg(6): C(21) /C(26) ring.

Table 6 Aromatic interaction parameters (Å and °) for description of π–π interaction in **ZnL_2** and **CuL_2**

Cg(I)–Cg(J)	$d_{\mathrm{Cg–Cg}}$[a]	α[b]	β, γ[c]	$d_{\mathrm{plane–plane}}$[d]	d_{offset}[e]	Symmetry codes
ZnL_2						
Cg(1)…Cg(3)	3.7361(15)	3.30(10)	23.89, 26.58	3.3413(8), 3.4161(10)	1.513, 1.672	-X,-Y,-Z
Cg(3)…Cg(1)	3.8016(15)	3.30(10)	25.09, 26.61	3.3989(8), 3.4428(10)	1.612, 1.703	-X,1-Y,-Z
CuL_2						
Cg(2)…Cg(4)	3.748(2)	2.99(16)	24.18, 26.62	3.3506(12), 3.4188(17)	1.679, 1.536	-X,1-Y,-Z
Cg(2)…Cg(4)	3.803(2)	2.99(16)	25.23, 26.61	3.3998(12), 3.4398(16)	1.366, 1.703	-X,2-Y,-Z

[a] Centroid–centroid distance. [b] Dihedral angle between the ring plane. [c] Offset angles: angle between Cg(I)–Cg(J) vector and normal to plane I, angle between Cg(I)–Cg(J) vector and normal to plane J (β = γ when α = 0). [d] Perpendicular distance of Cg(I) on ring J and perpendicular distance of Cg(J) on ring I. [e] Horizontal displacement between Cg(I) and Cg(J), two values if the two rings are not exactly parallel (α ≠ 0). For **ZnL_2** Cg(1): centroid of Zn(1)–O(1)–C(1)–C(6)–C(7)–N(1); Cg(2): centroid of C(1)–C(2)–C(3)–C(4)–C(5)–C(6). For **CuL_2** Cg(2): centroid of Cu(1)–O(2)–C(11)–C(16)–C(17)–N(2); Cg(4): centroid of C(11)–C(12)–C(13)–C(14)–C(15)–C(16).

Highlights

A bidentate Schiff base ligand (**HL**) was synthesized and characterized by different spectroscopic techniques.

VOL_2, **CoL_3, CuL_2 and ZnL_2** complexes were synthesized with the bidentate Schiff base ligand.

All the complexes were characterized by elemental analysis (CHN), FT-IR spectroscopy and single crystal X-ray diffraction technique.

ZnL_2 complex was investigated by NMR techniques.